Vapor-liquid equilibrium (VLE) measurements of ethanol – heptane at isothermal (363.15, 393.15 and 423.15 K) and isobaric (101.33 kPa) conditions and correlation of liquid viscosity data

Tomoya Tsuji [a,*], Hiroyuki Matsuda [b], Makoto Kawakita [b], Kiyofumi Kurihara [b], Katsumi Tochigi [b]

[a] Malaysia-Japan International Institute of Technology, Universiti Teknologi Malaysia, Off Jalan Sultan Yahya Petra, Kuala Lumpur 54100, Malaysia
[b] College of Science and Technology, Nihon University, 1-8-14 Kanda Surugadai, Chiyoda-ku, Tokyo 101-8308, Japan

ARTICLE INFO

ABSTRACT

Vapor-liquid equilibria (VLE) were measured for ethanol – heptane by a modified Rose-Williams equilibrium still combined with ebulliometer at three isotherms (363.15, 393.15 and 423.15 K) and an isobar (101.33 kPa). The azeotropes were observed in VLE, and the experimental data were correlated with the Peng-Robinson-Stryjek-Vera (PRSV) equation of state. The conventional mixing rule, with k_{ij} equal to zero calculates the azeotropic pressure close to the vapor pressure of ethanol. The Adachi-Sugie (AS) mixing rule provides 0.282% average absolute relative deviation (AARD) in temperature for isobaric VLE and 1.711% AARD for isothermal VLE. Eyring theory combined with the PRSV equation enabled an average of 2.810% AARD in correlation of literature liquid viscosity data, which is sufficient for considering biofuel injector. The method will be applied to flow analysis in general process design using mixtures because viscosity can be evaluated from equation of states.

1. Introduction

Electric vehicles (EVs) have received much attention as zero-local emission type of transportation. However, considering the present number of vehicles in the world, it is difficult to immediately switch from fuel-driven vehicles to EVs such that hybrid vehicles that use bioethanol blended with gasoline are being promoted in many countries. The volume percentage of ethanol in gasoline is given as an E-number, in which there are E5–10 grades in Europe, E10 and E15 grades in the U. S. and E18 to E27 grades in Brazil [1]. Bioethanol blended fuels are expected to be used in the future as fuels for vehicles. The physical properties, such as density, viscosity, heat capacity, and thermal conductivity, and phase equilibria are essential for design of biofuel injectors and their supply systems in gasoline engines [2–5]. Experimental vapor-liquid equilibria (VLE) data have been measured for ethanol and heptane mixtures by Katz and Newman [6] and Raal et al. [7]. Isothermal VLE and related data have been reported at 303 K [8, 9], at 298.15 K [10], 303 K [11], 303 K and 343 K [12], 313 K [13], 313 K [14, 15], 343 K, 353 K and 363 K [16], 483 K, 508 K and 523 K [17]. However, there are few reports in the temperature range from 353 K to 453 K, which is necessary for the design of direct fuel injector systems [2,3]. The authors have reported VLE data using equilibrium still and ebulliometer not only for systems under isobaric conditions, but also isothermal conditions [18–

22]. In this research, experimental techniques were applied for determination of isothermal VLE data of the ethanol - heptane system at 363 K to 423 K. To supplement the isothermal VLE measurements in this work, isobaric measurements were also measured at 101.33 kPa to validate the reliability of the data. In mechanical engineering, REFPROP has been widely used for the estimation of physical properties like phase equilibria, viscosity, heat capacity and thermal conductivity. However it is not always sufficient for mixtures containing polar substances. Therefore experimental data were correlated with the equation of state proposed by Styrjek and Vera [23], because it is reliable for calculating saturated vapor pressures of both hydrocarbons and alcohols. In this research, the equation of state was also applied to the estimation of viscosity by using Eyring theory. Methods that use Eyring theory for estimating viscosity from VLE data have been proposed [24–27]. Ono et al. [28] also employed the Eyring theory for estimating viscosity from P-V-T data in the liquid phase. Estimated viscosities from VLE data of this work were compared with those reported by Brunson and Byers [29].

1. Experimental section

2.1. Materials

Table 1 lists the chemicals used in this research. Ethanol and heptane were dehydrated with molecular sieve 3A before the measurements and

---

* Corresponding author at: Department of Applied Molecular Chemistry, Malaysia-Japan International Institute of Technology, Universiti Teknologi Malaysia, Off Jalan Sultan Yahya Petra, 54100 Kuala Lumpur, Malaysia.
E-mail address: t.tsuji@utm.my (T. Tsuji).

Table 1
Chemicals used in this study.

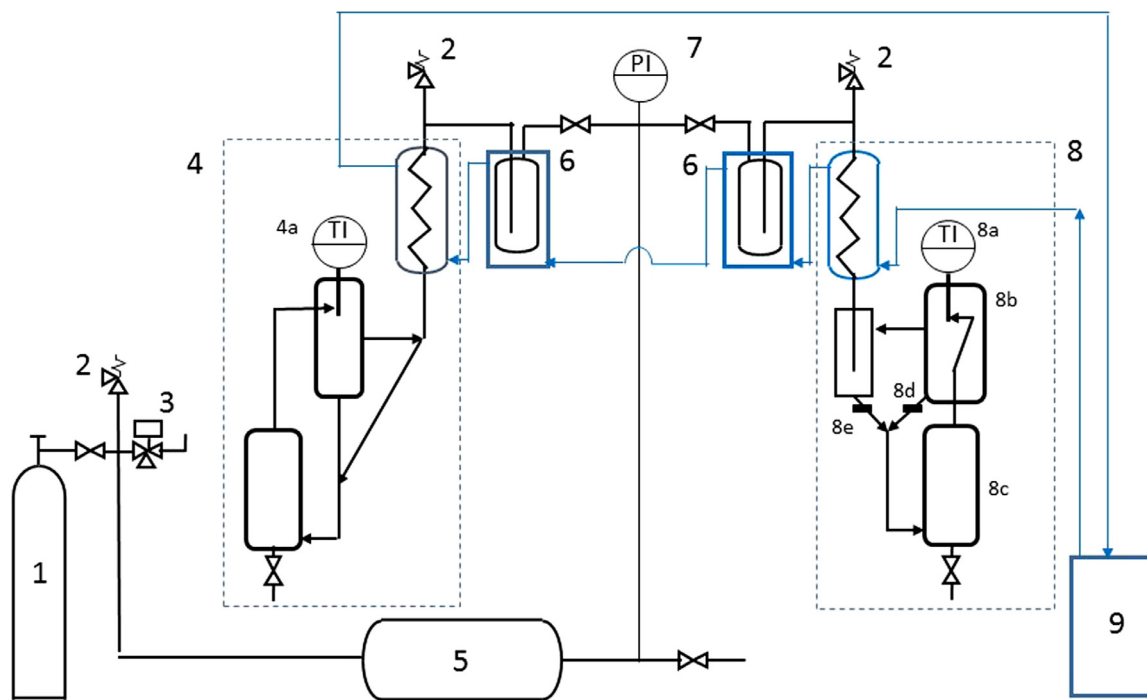|	CAS No.	Supplier	[a]Purity
Ethanol	64–17–5	Wako Pure Chemical Industries, Osaka, Japan	>99.9 wt%
Heptane	142–82–5	Wako Pure Chemical Industries, Osaka, Japan	>99.9 wt%

[a] Checked by gas chromatograph

Fig. 1. Schematic diagram of experimental apparatus; 1: Nitrogen cylinder; 2: Safety valve; 3: Solenoid valve; 4: Ebulliometer for reference / 4a: Pt resistance thermometer; 5: Surge tank; 6: Cold trap; 7: Pressure indicator; 8: Modified Rose-Williams equilibrium still for sample/ 8a: Pt resistance thermometer / 8b: Equilibrium chamber / 8c: Still / 8d,e: Sampling port; 9:Low temperature thermostatic bath.

purities were checked with a gas chromatograph. Peak areas of the impurities were no more than 0.1% for ethanol or heptane. Ion exchanged distilled water was used as a reference to determine experimental pressures at isothermal conditions.

2.2. Equipment and procedure

Fig. 1 shows the apparatus employed in this research with experimental procedures described in detail in previous reports [22]. The apparatus was composed of a modified Rose-Williams still, an ebulliometer for reference (part 4 in Fig. 1), a surge tank (part 5), a nitrogen cylinder (part 1), a low temperature thermostatic bath (part 9) and other equipment with the main parts of the apparatus being made of stainless steel 304. The apparatus was designed to have a safe working pressure of 5 MPa. The sample was heated up to about 483 K by a cartridge heater installed in the equilibrium still. In the procedure, the sample solution was loaded into the still of the ebulliometer (part 8c), and boiled under a given pressure. Then, the vapor and the liquid of the sample were sent together to the equilibrium chamber (part 8b). The liquid was returned to the still via the sampling port (part 8d). Otherwise, the vapor was sent to a Liebig condenser and liquefied. The liquefied vapor was returned to the still together with the liquid from the equilibrium chamber. In the apparatus operation, the number of drops from the condenser were ensured to be constant implying that the system was at steady-state and that the system was in the equilibrium. In isothermal VLE measurements, temperature was measured with a platinum resistance thermometer (part 8a), and pressure was evaluated from the temperature of pure water measured by another thermometer (part 4a). The two

thermometers were calibrated at the National Institute of Advanced Industrial Science and Technology (AIST), Japan. An equation, proposed by Bridgeman and Aldrich [30], was employed for evaluation of pressure balance with that of the ebulliometer for the sample. A small portion of the liquid phase and of the liquefied vapor phase were taken from sampling ports (parts 8d and 8e) using a gastight syringe, and the composition was analyzed with a gas chromatograph (Shimadzu GC-4BT, Kyoto, Japan) equipped with a thermal conductivity detector. The column packing was PEG-1500, 15% polyethylene glycol on Uniport, 60/80 mesh (Gasukuro Kogyo, Tokyo). In the isobaric VLE measurements, the system was at atmospheric pressure and the temperature was measured solely by the thermometer (part 8a), while the ebulliometer was not used.

In the isobaric measurements, the temperature measured was corrected to that at 101.33 kPa via:

$$T = T_{meas} + \frac{1}{(\ln 10) \sum_i \frac{x_i B_i}{(T_{meas}+C_i)^2}} \times \frac{101.33 - p_{atm,meas}/kPa}{p_{atm,meas}/kPa} \quad (1)$$

where T_{meas} is the temperature measured under atmospheric pressure, $p_{atm,meas}$, x_i is the mole fraction of liquid phase. B_i and C_i are constants in the following Antione equation:

$$\ln p^s_i = A_i - \frac{B_i}{T/K - C_i} \quad (2)$$

where constants, A_i, B_i and C_i, were determined from the experimental saturated vapor pressure data of ethanol and heptane. Considering that the thermometer calibration and thermal oscillation of the system, uncertainty of temperature was estimated to be $u(T)$=0.06 K.

Table 2
Critical properties used for PRSV equation [23].

	Critical temperature T_c /K	Critical pressure p_c / kPa	Acentric factor ω /-	κ_1 /-
Ethanol	513.92	6148	0.64439	−0.03374
Heptane	540.10	2735.75	0.35022	0.04648

Considering the peak area in gas chromatogram, uncertainties in mole fraction for vapor and liquid were estimated to be $u(x_i)=u(y_i)=0.003$, respectively. The uncertainty of pressure depended on the temperature of water in the ebulliometer, because the value of pressure was determined by the equation of Bridgeman and Aldrich [30]. For example, the uncertainties of pressure at (100, 500, 1000, 2000) kPa were evaluated to be $u(p)=$ (0.25, 0.70, 1.20, 2.43) kPa, respectively.

3. Correlation

3.1. VLE correlation

The modified Peng-Robinson equation of state of Stryjek and Vera (PRSV) [23] was employed for correlation of VLE data:

$$p = \frac{RT}{v-b} - \frac{a}{v^2 + 2bv - b^2} \tag{3}$$

where parameters, a and b, were evaluated from the critical temperature, T_c, critical pressure, p_c, acentric factor, ω, and an additional parameter, κ_1 [23]. The additional parameter κ_1 was proposed for well representing the saturated vapor pressure data [23]. Considering the azeotrope reported in ethanol –heptane [8–17], the good reproducibility is essential for saturated vapor pressure to determine the binary parameters in the mixing rule. **Table 2** lists the parameters used in the calculations. Some mixing rules should be considered for the correlation of VLE data, because van der Waals one fluid model does not always provide azeotropes. It is well known that mixing rules, based on excess free energy models [31–33], are employed for correlating the systems with complex phase behavior. However, the estimation of VLE and viscosity are considered for design of biofuel injectors in gasoline engine. Then, complex mathematical functions are not useful for estimation of heat capacities. Though estimation of heat capacity were not discussed in this research, mixing rules with simple mathematical function will be preferable. Therefore, mixing rules proposed by Adachi and Sugie (AS) were employed, since these also allow description of polar-nonpolar systems [34]:

$$a = \sum_i \sum_j x_i x_j \left[1 - k_{ij} + l_{ij}(x_i - x_j)\right] \left(a_i a_j\right)^{1/2} \tag{4}$$

$$b = \sum_i \sum_j x_i x_j \frac{b_i + b_j}{2} \tag{5}$$

where k_{ij} and l_{ij} are two binary parameters. It should be noted that the functional form of Eq. (4) is similar to that of a Margules type activity coefficient model. In this research, the binary parameters were determined from fitting isothermal VLE data. Several combinations of (k_{ij}, l_{ij}) were obtained to provide the azeotropic point at first and successively, with final values being determined by minimizing the following objective function:

$$O.F. = \sum (x_1 - x_{1,\text{calc}}) \tag{6}$$

After identifying the temperature dependence in k_{ij} and l_{ij}, the isobaric VLE were calculated.

3.2. Estimation of liquid viscosity

According to Eyring theory [35], the liquid viscosity of the binary mixture, η, at given temperature, T, and pressure, p, is given as follows:

$$\ln \eta v = x_1 \ln \left[\eta_1^\circ(T,p)v_1^\circ(T,p)\right] + x_2 \ln \left[\eta_2^\circ(T,p)v_2^\circ(T,p)\right] + \frac{E_a}{RT} \tag{7}$$

where v_i° is the molar volume, η_i° is the viscosity of pure component i and E_a is the activation energy that can be assumed to be proportional to the excess Gibbs energy, G^E:

$$E_a = \sigma G^E \tag{8}$$

where σ is a constant that depends on the system and G^E is defined as follows:

$$\frac{G^E}{RT} = x_1 \ln \frac{f_1(T,p)}{x_1 f_1^\circ(T,p)} + x_2 \ln \frac{f_2(T,p)}{x_2 f_2^\circ(T,p)} \tag{9}$$

where f_i° and f_i are the fugacities of component i as a pure substance and as a component in the mixture, respectively. In this research, v, v_i°, f_i° and f_i were estimated with the PRSV equation.

3.3. Deviations and absolute relative deviations

The relative deviations (RDs) and the absolute relative deviations (ARDs) were evaluated as follows:

$$(RD) \quad \frac{\Delta X}{X_{exp}} = \frac{X - X_{exp}}{X_{exp}} \tag{10}$$

$$(ARD) \quad \frac{|\Delta X|}{X_{exp}} = \frac{|X - X_{exp}|}{X_{exp}} \tag{11}$$

Sparacwhere X and X_{exp} refer to calculated and experimental properties. For saturated pressures, X corresponds to that of the Antoine equation p_{fit}^s or that of the PRSV equation p_{cal}^s at a given temperature. For isothermal VLE, X is the pressure given by the PRSV equation at a given mole fraction x_1 and mole fraction y_1 at given pressure p. For isothermal VLE, X is the temperature at a given mole fraction x_1 and mole fraction y_1 at a given temperature T. For the estimation of viscosity, X is the viscosity η at a given mole fraction x_1.

4. Result and discussion

4.1. Saturated vapor pressure

Table 3 gives the saturated vapor pressures for ethanol and heptane. The experimental pressure should be higher than atmospheric pressure in the apparatus employed, so the experimental temperatures ranged from (351.48 to 463.08) K and (371.82 to 483.15) K for ethanol and heptane, respectively. The data for ethanol agreed with the standard data of Schroder et al. [36], and those for heptane agreed with values reported by National Institute of Standard and Technology (NIST) [37]. The constants in the Antoine equation, Eq. (2), were determined by fitting experimental vapor pressure data (**Table 4**). The RDs are shown in **Fig. 2** and the average absolute relative deviation (AARDs) were 0.295% and 0.270% for the experimental data of ethanol and heptane, respectively. The AARDs were also calculated for the literature data ethanol and the standard data of heptane. The AARD for the literature data of ethanol were 0.471%. The AARD for the standard data of heptane was calculated for every 0.15 K from 371.85 K to 383.20 K in the NIST Chemistry WebBook, and the AARD was 0.180%. Constants in the Antoine equation were used in the isobaric VLE to correct the pressure from atmospheric pressure at measurement to 101.33 kPa.

Table 3
Saturated vapor pressure for ethanol(1) and heptane(2).

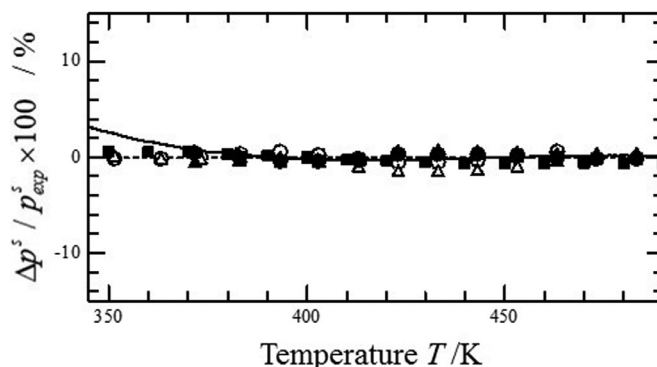| Measured		Antoine equation			PRSV equation		
[a]Temperature	[b]Pressure	Pressure			Pressure		
T /K	p^s /kPa	p^s_{fit} /-	[c]Δp^s /-	[d]$|\Delta p^s|/p^s_{exp}$ /%	p^s_{cal} /-	[e]Δp^s /-	[f]$|\Delta p^s|/p^s_{exp}$ /%
Ethanol (1)							
351.48	101.77	101.61	−0.16	0.160	101.77	0.00	0.000
363.15	158.48	158.26	−0.22	0.140	158.00	−0.48	0.303
373.15	225.21	225.24	0.03	0.013	224.55	−0.66	0.293
383.15	312.45	313.52	1.07	0.341	312.04	−0.41	0.131
393.22	426.23	428.57	2.34	0.548	425.78	−0.45	0.106
403.15	571.38	572.73	1.35	0.236	568.02	−3.36	0.588
413.15	755.33	754.21	−1.12	0.148	746.81	−8.52	1.128
423.16	983.30	978.27	−5.03	0.512	967.38	−15.92	1.619
433.20	1257.89	1251.92	−5.97	0.475	1236.86	−21.03	1.672
443.14	1582.62	1577.65	−4.97	0.314	1558.13	−24.49	1.547
453.14	1966.01	1967.21	1.20	0.061	1943.47	−22.54	1.146
463.08	2408.79	2422.90	14.11	0.586	2396.22	−12.57	0.522
		average	0.22	0.295	average	−9.20	0.755
Heptane (2)							
371.82	102.53	102.97	0.44	0.431	101.92	−0.61	0.595
382.99	140.68	140.57	−0.11	0.077	139.95	−0.73	0.519
393.16	184.39	183.58	−0.81	0.438	183.22	−1.17	0.635
403.10	236.03	235.02	−1.01	0.428	234.94	−1.09	0.462
413.22	299.21	298.31	−0.90	0.299	298.51	−0.70	0.234
423.15	371.21	372.54	1.33	0.359	373.00	1.79	0.482
433.15	459.10	460.90	1.80	0.391	461.63	2.53	0.551
443.15	562.77	564.43	1.66	0.294	565.48	2.71	0.482
453.16	683.67	684.82	1.15	0.168	686.34	2.67	0.391
463.15	823.31	823.28	−0.03	0.003	825.53	2.22	0.270
473.15	983.16	981.81	−1.35	0.138	985.27	2.11	0.215
483.15	1164.39	1161.88	−2.51	0.215	1167.34	2.95	0.253
		average	−0.03	0.270	average	1.06	0.424

[a] $u(T)=0.06$ K

[b] $u(p^s)$ depends on the pressure range, 0.25 kPa (at 100.00 kPa), 0.70 kPa (at 500.00 kPa), 1.20 kPa (at 1000.00 kPa) and 2.43 kPa (at 2000.00 kPa)

[c] $\Delta p^s = p^s_{fit} - p^s_{exp}$

[d] $|\Delta p^s|/p^s_{exp} = \frac{|p^s_{fit} - p^s_{exp}|}{p^s_{exp}} \times 100$

[e] $\Delta p^s = p^s_{cal} - p^s_{exp}$

[f] $|\Delta p^s|/p^s_{exp} = \frac{|p^s_{cal} - p^s_{exp}|}{p^s_{exp}} \times 100$

Table 4
Constants in Antoine equation determined from data in Table 3.

	Constants in [a]Antoine equation			Temperature range	
	A_i /-	B_i /K	C_i /K	T_{min} / K	T_{max} / K
Ethanol (1)	15.9114	3225.34	−65.81	351.48	463.08
Heptane (2)	14.5964	3450.11	−25.49	371.82	483.15

[a] $\ln p^s_i/kPa = A_i - \frac{B_i}{T/K+C_i}$

4.2. Isobaric VLE

Table 5 lists experimental data of VLE for ethanol (1) - heptane (2) at 101.33 kPa. The thermodynamic consistency test, proposed by Ferdenslund et al. [38, 39], was carried out for the experimental data, and its reliability was ensured. Detailed descriptions are given in **Supplemental Materials 1**. **Fig. 3** shows isobaric VLE along with the data of Katz and Newman [6], and Raal et al. [7] at 760 mmHg (101 kPa). The experimental temperatures rapidly decreased in mole fraction of ethanol up to x_1=0.150. Though Katz and Newman [6] reported constant temperatures in the mole fraction of ethanol from 0.489 to 0.791, the experimental data and those of Raal et al. [7] showed a lower temperature. The VLE data were considered to be showing an azeotrope in this work. The azeotropic point is sometimes affected by a small amount of water in ethanol, and can changed into a heterogeneous azeotrope.

Fig. 2. RDs for saturated vapor pressure of ethanol and heptane; (○): ethanol for Antoine equation; (●): heptane for Antoine equation; (△): ethanol for PRSV equation; (▲): heptane for PRSV equation; (■): ethanol (Schroder et al. [33]) for Antoine equation;(———-) : heptane (NIST Chemistry WebBook [34]) for Antoine equation.

Though it is difficult to check heterogeneous phases in the present apparatus, cloudy solutions indicative of heterogeneous azeotropy were not observed in the measurements. Using the experimental data, the azeotropic point was determined by plots of $y_1 - x_1$, and an equation for the temperature by using Lagrange interpolation. The azeotropic point determined is listed in **Table 6**.

Table 5
Isobaric VLE for ethanol (1) - heptane (2) at [a]101.33 kPa.

Measured			PRSV equation (at $x_{1,exp}$)					
[b]Temperature	[c]Mole fraction of ethanol		Temperature			Mole fraction of ethanol in vapor phase		
	(Liquid)	(Vapor)						
T /K	x_1 /-	y_1 /-	T_{cal} /-	[d]ΔT /	[e]$|\Delta T|/T_{exp}$ /%	$y_{1,cal}$ /-	[f]Δy_1 /-	[g]$|\Delta y_1|/y_{1,exp}$ /%
349.18	0.080	0.513	353.74	4.56	1.307	0.457	−0.056	10.949
348.22	0.107	0.530	351.23	3.01	0.864	0.509	−0.021	3.901
346.08	0.175	0.578	347.63	1.55	0.446	0.582	0.004	0.730
345.46	0.248	0.596	345.94	0.48	0.140	0.618	0.022	3.609
345.29	0.273	0.600	345.63	0.34	0.099	0.625	0.025	4.097
345.00	0.365	0.606	345.07	0.07	0.020	0.639	0.033	5.457
344.62	0.472	0.620	344.92	0.30	0.086	0.644	0.024	3.941
344.53	0.561	0.634	344.89	0.36	0.103	0.647	0.013	1.975
344.48	0.651	0.648	344.87	0.39	0.113	0.652	0.004	0.572
344.46	0.691	0.653	344.88	0.42	0.121	0.656	0.003	0.453
344.95	0.821	0.702	345.30	0.35	0.103	0.696	−0.006	0.888
345.66	0.887	0.745	346.15	0.49	0.142	0.746	0.001	0.108
346.26	0.918	0.779	346.88	0.62	0.180	0.784	0.005	0.622
346.86	0.942	0.811	347.70	0.84	0.242	0.824	0.013	1.606
347.67	0.961	0.847	348.56	0.89	0.257	0.866	0.019	2.214
			average	0.978	0.282	average	0.005	2.741

[a] $u(p)$=0.25 kPa
[b] $u(T)$=0.06 K
[c] $u(x_1)=u(y_1)$=0.003
[d] $\Delta T = T_{cal} - T_{exp}$
[e] $|\Delta T|/T_{exp} = \frac{|T_{cal}-T_{exp}|}{T_{exp}} \times 100$
[f] $\Delta y_1 = y_{1,cal} - y_{1,exp}$
[g] $|\Delta y_1|/y_{1,exp} = \frac{|y_{1,cal}-y_{1,exp}|}{y_{1,exp}} \times 100$

Table 6
Measured and calculated azeotropes for ethanol(1) - heptane(2).

Type of data	Measured			PRSV equation		
	Mole fraction of ethanol $x_{1,az}$ /-	Temperature T_{az} /K	Pressure p_{az} /kPa	Mole fraction of ethanol $x_{1,az}$ /-	Temperature T_{az} /K	Pressure p_{az} /kPa
Isobaric	0.645	344.48	[a]101.33	0.651	344.87	[a]101.33
Isothermal	0.715	[a]363.15	199.55	0.680	[a]363.15	198.65
Isothermal	0.749	[a]393.15	497.41	0.734	[a]393.15	494.23
Isothermal	0.781	[a]423.15	1066.47	0.745	[a]423.15	1069.17

[a] fixed at measurement

4.3. Isothermal VLE

Table 7 lists experimental VLE data for ethanol (1) – heptane (2) at (363.15, 393.15, 423.15) K. **Fig. 4** shows isothermal VLE along with data reported by Ramalho and Delmas [16] at 343 K and 363 K, Berro et al. [12] at 343.17 K, and Seo et al. [17] at 483.15 K. The VLE data of the five isotherms had similar tendencies, however, the experimental pressures at 363.15 K were slightly lower than those of Ramalho and Delmas [16] at 363 K. The pressures in the data of Berro et al. [12] were also lower than those of Ramalho and Delmas [16] at 343 K. Ramalho and Delmas [16], and Berro et al. [12] measured VLE with an equilibrium still, while Seo et al. [17] made measurements with a high-pressure cell equipped with circulation pumps. When heat insulation of the equilibrium chamber is not sufficient in the equilibrium still, then the measured temperature probably tends to be slightly high, however, detailed discussion on this point is not possible here. The azeotropic points are shown in **Table 6**. The mole fraction of ethanol at the azeotropic point shifted to be larger with increasing temperature (**Table 6**). According to Seo et al. [17], the azeotropic point is separated by two points at high temperatures.

4.4. Calculation of saturated vapor pressure with PRSV equation

Prior to VLE correlation, reproducibility of the PRSV equation was checked for reliability of calculating experimental saturated vapor pres-

sure data. **Table 3** lists the calculation results and **Fig. 2** shows the RDs, which were all negative for ethanol over the entire range of temperatures. The largest RD in PRSV calculation of vapor pressure was found around 433 K. Even though the RDs for PRSV were larger than those for the Antoine equation, the AARD (**Table 3**) was 0.755%. The sign of the RDs for PRSV changed from negative to positive for heptane, with deviatios being smaller than those for ethanol and having the AARD (**Table 3**) of 0.424%.

4.5. Correlation of VLE

At first, VLE at 393.15 K was correlated with conventional mixing rules setting l_{12}=0.000 (**Supplemental Materials 2**). For k_{12}=0.000, the azeotropic point was calculated to be at a mole fraction close to ethanol, otherwise, k_{12}=0.170 provided reproducibility only at a mole fraction close to heptane, suggesting that at least two parameters are necessary in the mixing rules. It is well known that binary parameters, k_{12} and l_{12}, can have temperature dependence, so their values were determined separately by fitting the data at three temperature (**Table 8**). **Table 7** and **Fig. 4** compare calculated results with the data and **Table 6** shows calculated azeotropic points with the PRSV equation. **Fig. 5** shows the RDs for pressures and vapor phase mole fractions with the correlation mainly being carried out to reproduce the azeotropic point. An enlargement of composition ranges around the azeotrope is shown in **Fig. 5** for which the AARDs (**Table 7**) for pressure were 2.457%, 1.392% and 1.340%

Table 7

Isothermal VLE for ethanol (1) - heptane (2) at 363.15, 393.15 and 423.15 K.

Measured [a]Pressure	[b]Mole fraction of ethanol (Liquid)	(Vapor)	PRSV equation at $x_{1,exp}$ Pressure			Mole fraction of ethanol in vapor		
p /kPa	x_1 /-	y_1 /-	p_{cal} /kPa	[c]Δp /kPa	[d]$|\Delta p|/p_{exp}$ /%	$y_{1,cal}$ /-	[e]Δy_1/-	[f]$|\Delta y_1|/y_{1,exp}$ /%
[g]363.15 K								
152.58	0.070	0.500	133.18	−19.40	12.712	0.434	−0.066	13.143
173.62	0.122	0.580	157.95	−15.67	9.023	0.536	−0.044	7.531
181.52	0.171	0.608	173.15	−8.37	4.608	0.587	−0.021	3.450
185.92	0.213	0.628	181.84	−4.08	2.193	0.614	−0.014	2.267
189.26	0.277	0.648	189.97	0.71	0.376	0.637	−0.011	1.755
193.41	0.368	0.667	195.35	1.94	1.004	0.657	−0.010	1.567
194.97	0.458	0.680	197.32	2.35	1.207	0.665	−0.015	2.223
197.47	0.533	0.692	197.94	0.47	0.240	0.669	−0.023	3.314
198.38	0.615	0.701	198.48	0.10	0.050	0.674	−0.027	3.824
199.44	0.686	0.708	198.65	−0.79	0.396	0.679	−0.029	4.086
199.43	0.750	0.719	198.25	−1.18	0.590	0.694	−0.025	3.505
198.66	0.805	0.730	196.84	−1.82	0.918	0.712	−0.018	2.463
191.98	0.879	0.782	191.53	−0.45	0.236	0.757	−0.025	3.153
184.69	0.930	0.832	183.13	−1.56	0.846	0.817	−0.015	1.781
			average	−3.41	2.457	average	−0.024	3.862
[g]393.15 K								
249.31	0.028	0.273	237.08	−12.23	4.905	0.232	−0.041	14.970
421.18	0.182	0.614	405.08	−16.10	3.822	0.577	−0.037	5.966
449.30	0.289	0.637	450.87	1.57	0.350	0.637	−0.036	5.291
465.67	0.367	0.702	468.30	2.63	0.565	0.659	−0.043	6.068
474.57	0.448	0.713	479.23	4.66	0.982	0.676	−0.037	5.135
485.92	0.542	0.726	487.08	1.16	0.239	0.693	−0.033	4.602
490.02	0.608	0.732	490.82	0.80	0.163	0.704	−0.028	3.804
494.87	0.672	0.736	493.28	−1.59	0.322	0.717	−0.019	2.544
497.08	0.721	0.742	494.18	−2.90	0.583	0.730	−0.012	1.643
497.16	0.781	0.759	493.43	−3.73	0.750	0.750	−0.009	1.159
495.60	0.837	0.785	489.51	−6.09	1.228	0.778	−0.007	0.938
481.14	0.920	0.845	472.05	−9.09	1.888	0.848	0.003	0.317
475.12	0.940	0.870	464.18	−10.94	2.302	0.874	0.004	0.467
			average	−3.99	1.392	average	−0.023	4.070
[g]423.15 K								
887.61	0.135	0.602	798.78	−88.85	10.010	0.526	−0.076	12.597
921.08	0.194	0.642	885.23	−35.85	3.892	0.577	−0.065	10.162
942.85	0.242	0.666	931.70	−11.15	1.182	0.602	−0.064	9.595
953.92	0.277	0.679	956.59	2.67	0.280	0.616	−0.063	9.323
970.79	0.316	0.696	978.12	7.33	0.756	0.628	−0.068	9.790
989.43	0.373	0.714	1001.70	12.27	1.240	0.642	−0.072	10.051
1012.13	0.450	0.729	1024.78	12.65	1.250	0.659	−0.070	9.637
1042.13	0.547	0.750	1046.33	4.20	0.403	0.680	−0.070	9.368
1050.05	0.601	0.753	1055.81	5.76	0.548	0.693	−0.060	7.924
1055.93	0.652	0.760	1062.95	7.02	0.665	0.708	−0.052	6.778
1062.24	0.717	0.769	1068.49	6.25	0.589	0.733	−0.036	4.725
1065.75	0.757	0.775	1069.05	3.30	0.310	0.740	−0.035	4.459
1065.65	0.812	0.789	1064.67	−0.98	0.092	0.783	−0.006	0.718
1062.67	0.843	0.804	1058.68	−3.99	0.375	0.806	0.002	0.217
1052.09	0.882	0.834	1046.57	−5.52	0.524	0.840	0.006	0.714
1033.03	0.920	0.873	1028.80	−4.23	0.410	0.879	0.006	0.713
1019.90	0.939	0.897	1017.34	−2.56	0.251	0.904	0.007	0.755
			average	−5.39	1.340	average	−0.042	6.325

[a] $u(p)$ depends on the pressure range, 0.70 kPa (at 500.00 kPa) and 1.20 kPa (at 1000.00 kPa)

[b] $u(x_1)=u(y_1)=0.003$

[c] $\Delta p = p_{cal} - p_{exp}$

[d] $|\Delta p|/p_{exp} = \frac{|p_{cal} - p_{exp}|}{p_{exp}} \times 100$

[e] $\Delta y_1 = y_{1,cal} - y_{1,exp}$

[f] $|\Delta y_1|/y_{1,exp} = \frac{|y_{1,cal} - y_{1,exp}|}{y_{1,exp}} \times 100$

[g] $u(T)=0.06$ K

for 363.15 K, 393.15 K and 423.15 K, respectively, while those for mole fraction in the vapor phase were 3.862%, 4.070% and 6.325%, respectively. Especially, RDs were larger at small mole fractions of ethanol in the liquid phase. Calculations were carried out for the data of Berro et al. [12] at 343.15 K and Seo et al. [17] at 483.15 K. The fitted values of k_{12} and l_{12} are listed in Table 8, and the calculation results are shown in Fig. 4. The calculation results agreed well the experimental data for mole fractions in liquid phase at 483.15 K (Fig. 4). Otherwise, the cal-

culated mole fractions in the vapor phase (Fig. 4) had higher deviations compared with those in liquid phase. The temperature dependence of k_{12} and l_{12} were determined to be as follows:

$$k_{12} = 1.3193 - 1.1204 \times 10^{-3} T/K - \frac{291.78}{T/K} \quad (12)$$

$$l_{12} = -25.572 + 6.5240 \times 10^{-2} T/K - 5.4600 \times 10^{-5} (T/K)^2 + \frac{3322.1}{T/K} \quad (13)$$
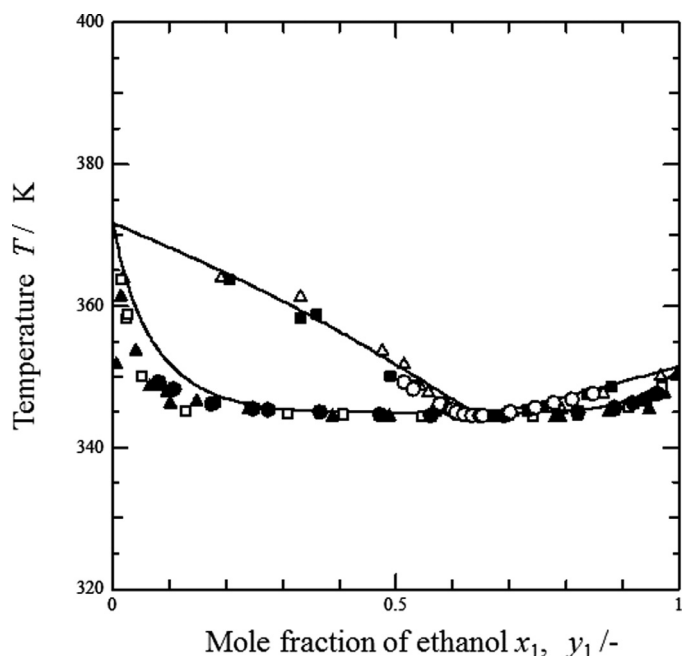
Fig. 3. Isobaric VLE for ethanol (1) – heptane (2) at 101.33 kPa; (●, ○): This work; (▲, △): Katz and Newman [6], 101 kPa; (□, ■): Raal et al. [7], 101 kPa;(——-) : PRSV equation.
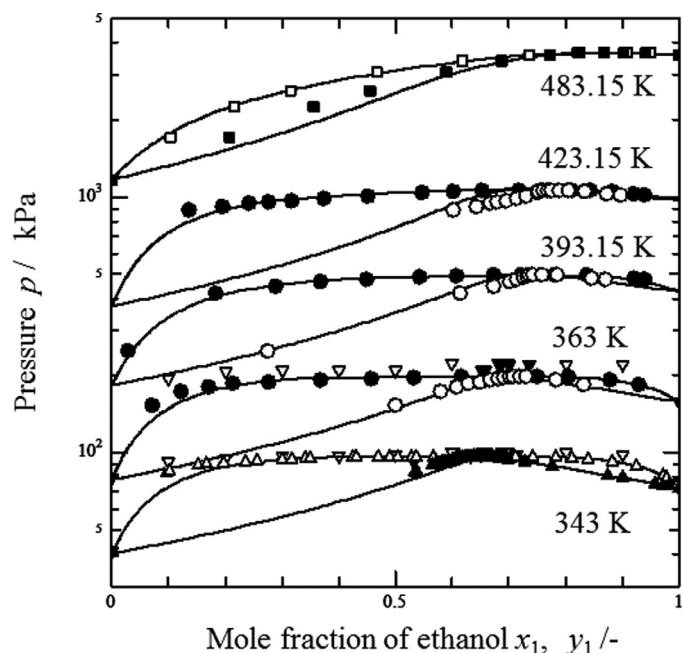

Fig. 4. Isothermal VLE for ethanol (1) – heptane (2) at (343 to 483) K; (●, ○): This work, 363.15, 393.15, 423.15 K; (▼,▽): Ramaloh and Delmas [16], 343, 363 K; (▲,△): Berro et al. [12], 343.17 K; (□, ■): Seo et al. [17], 483.15 K; (——-): PRSV equation.

Table 8

Parameters in AS mixing rule and coefficients for molar Gibbs energy in Eyring equation.

Temperature T /K	Parameters in AS mixing rule		Coefficient for molar Gibbs energy (T-dependent) σ /-
	$k_{12}(=k_{21})$ /-	$l_{12}(=-l_{21})$ /-	
343.17	0.087	0.059	
363.15	0.108	0.069	0.08
393.15	0.128	0.072	−0.09
423.15	0.165	0.105	−0.28
483.15	0.172	0.068	

Fig. 5. RDs of VLE from calculation by PRSV equation for ethanol (1) – heptane (2); (○): 363.15 K; (●): 393.15 K; (□): 423.15 K; (+): 101.33 kPa.

Using Eqs. (12)-(13), isobaric VLE were calculated at 101.33 kPa (Fig. 3). Tables 5 and 6 provides a summary of calculated results. Fig. 5 shows the RDs for temperature and vapor phase mole fraction. The AARDs (Table 5) were 0.282% and 2.741% for the temperature and the mole fraction in the vapor phase, respectively. Though the reproducibility was poor at low mole fractions in vapor phase, the calculations agreed with the experimental data including the azeotrope.

4.6. Correlation of viscosity

Brunson and Byers have reported the liquid viscosity for ethanol (1) – heptane (2) with dynamic laser light scattering technique [29], that seems to be at conditions close to the saturation pressure. Measurements were carried out at mole fractions of ethanol of x_1 =0.0, 0.3, 0.5, 0.8, 0.9 and 1.0. In this research, values of viscosity at 363.15 K, 393.15 K and 423.15 K, were obtained by interpolation of literature data. In the interpolation, the functional form of the viscosity at a given mole fraction, was assumed to be cubic in inverse temperature:

$$\ln \eta_{est}(T, p, x_1) = a_{vis0, x_1} + a_{vis1, x_1}\left(\frac{1}{T}\right) + a_{vis2, x_1}\left(\frac{1}{T}\right)^2 + a_{vis3, x_1}\left(\frac{1}{T}\right)^3 \tag{14}$$

Viscosity data were calculated by using the PRSV equation combined with Eyring theory. In Eq. (7), the viscosity of pure ethanol or heptane, $\eta_{est,i}°(T, p)$ at a given pressure, p, was not available. Therefore, the following assumptions were employed:

$$\eta_{est,i}°(T, p) = \eta_{est}(T, p_i^s, x_i = 0) \quad (i = 1, 2) \tag{15}$$

Table 9

Estimated and calculated liquid phase viscosities for ethanol (1) – heptane (2) at isothermal conditions.

Mole fraction of ethanol x_1 /-	[a]Estimated viscosity η_{est} /mPa·s	Calculated viscosity σ=0.05 /-			T-dependent σ		
		η_{cal} /mPa·s	[b]Δη /mPa·s	[c]|Δη|/η_{est} /%	η_{cal} /mPa·s	[b]Δη /mPa·s	[c]|Δη|/η_{est} /%
363.15 K							
0.0	0.198						
0.3	0.221	0.232	0.011	5.081	0.220	−0.001	0.295
0.5	0.254	0.266	0.012	4.561	0.249	−0.005	1.902
0.8	0.337	0.346	0.009	2.668	0.332	−0.005	1.412
0.9	0.375	0.386	0.011	3.018	0.377	0.002	0.683
1.0	0.438						
		average	0.011	3.832	average	−0.003	1.073
393.15 K							
0.0	0.160						
0.3	0.167	0.173	0.006	3.778	0.176	0.009	5.043
0.5	0.193	0.189	−0.004	2.313	0.196	−0.003	0.564
0.8	0.239	0.231	−0.008	3.174	0.234	−0.005	1.869
0.9	0.257	0.254	−0.003	1.046	0.256	−0.001	0.228
1.0	0.284						
		average	−0.002	2.578	average	0.000	1.926
423.15 K							
0.0	0.134						
0.3	0.130	0.130	0.000	0.312	0.141	0.011	8.879
0.5	0.141	0.134	−0.007	4.937	0.147	0.006	3.697
0.8	0.174	0.156	−0.018	10.283	0.165	−0.009	5.317
0.9	0.182	0.169	−0.013	6.875	0.175	−0.007	3.838
1.0	0.187						
		average	−0.009	5.602	average	−0.001	5.433

[a] interpolated data of Bernson and Byers [29].

[b] $|\Delta\eta|/y_{1,exp} = \frac{|\eta_{cal}-\eta_{est}|}{\eta_{est}} \times 100$

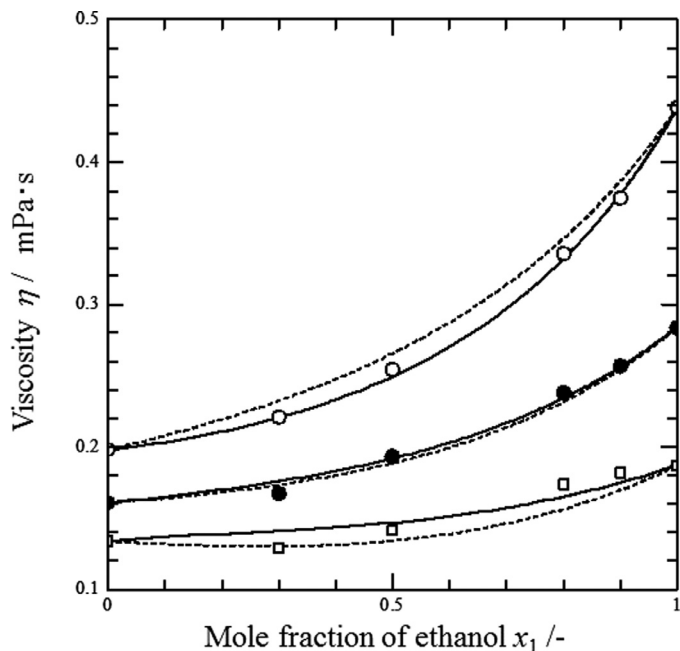[c] $\Delta\eta = \eta_{cal} - \eta_{est}$

Fig. 6. Liquid viscosity for ethanol (1) – heptane (2);(○, ●, □): Brunson and Byers [29], 363.15, 393.15, 423.15 K (interpolated); (——): PRSV equation with σ=0.05; (——): PRSV equation with $\sigma = 5.7055 - 1.0384 \times 10^{-2}T/K - \frac{673.49}{T/K}$.

where $\eta_i(T, p_i^s, x_i = 0)$ is the viscosity at the saturated vapor pressure of pure ethanol (1) or heptane (2), and available in the literature [29]. In Eq. (8), the parameter σ was determined under the temperature independent and dependent assumptions. The temperature independent parameter was σ=−0.05. The parameters, separately fitted with the viscosity data at 363.15 K, 393.15 K and 423.15 K, were listed in Table 8. Calculated viscosity values are shown in Fig. 6 and Table 9. The temper-
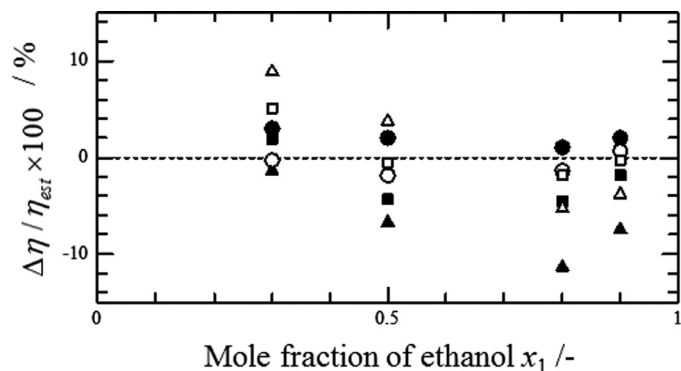

Fig. 7. RDs of viscosity from calculation by PRVV equation for ethanol (1) – heptane (2); (○): 363.15 K, σ=0.08; (□): 393.15 K, σ=−0.09; (△): 423.15 K, σ=−0.28; (●): 363.15 K, σ=0.05; (■): 393.15 K, σ=0.05; (▲): 423.15 K, σ=0.05.

ature dependent parameters provided better agreements with the liquid viscosity data than those with the temperature independent parameter especially in low temperature range. The temperature dependence of σ was given by:

$$\sigma = 5.7055 - 1.0384 \times 10^{-2}T/K - \frac{673.49}{T/K} \qquad (16)$$

Though some deviations were found in the calculation at 423.15 K, it seems to be related to system oscillations. The AARDs (Fig. 7) with σ=−0.05 were 3.832%, 2.578% and 5.602% at 363.15 K, 393.15 K and 423.15 K, respectively. Otherwise, those with Eq. (16) were 1.073%, 1.926% and 5.433% at 363.15 K, 393.15 K and 423.15 K, respectively.

5. Conclusions

Vapor-liquid equilibria data were measured for binary mixtures of ethanol – heptane with a modified Rose-Williams equilibrium still at one isobar and at three isotherms, (363 to 423) K, corresponding to conditions for direct fuel injection into gasoline engines. The PRSV equation

and the Adachi-Sugie mixing rules provided correlation of the data except at ethanol mole fractions lower than 0.25. Combination of Eyring theory with an additional parameter, σ, allowed estimation of liquid viscosity data at (363 to 423) K. The data and correlation are useful for the design of direct fuel injectors that use bioethanol blended gasolines. Considering corresponding state correlations for transport properties, the methods outlined in this paper can probably be extended to the correlation of thermal conductivities and diffusion coefficients of bioethanol - gasoline mixtures.

Credit authorship contribution statement

Tomoya Tsuji: Calculation, Collection and analysis of literature, Data analysis, Writing - Review & Editing. **Hiroyuki Matsuda**: Methodology, Investigation, Writing - Review & Editing. **Makoto Kawakita**: Investigation, Writing- Original Draft. **Kiyofumi Kurihara**: Design of equilibrium still and ebulliometer, Co-supervision of MK. **Katsumi Tochigi**: Overall Planning, Data analysis, Supervision of MK.

Declaration of Competing Interest

The authors declare that they have no conflicts of interest with the contents of this article.

The authors declare that they have no known competing financial interests or personal relationships that could have appeared to influence the work reported in this paper.

Supplementary materials

Supplementary material associated with this article can be found, in the online version, at doi:10.1016/j.ctta.2022.100041.

References

[1] L. Jęczmionek, B. Danek, M. Pałuchowska, W. Krasodomski, Changes in the Quality of E15–E25 Gasoline during Short-Term Storage up to Four Months, Energy Fuels 31 (2017) 504–513, doi:10.1021/acs.energyfuels.6b01260.

[2] N. Sharma, A.K. Agarwal, Effect of the Fuel Injection Pressure on Particulate Emissions from a Gasohol (E15 and M15)-Fueled Gasoline Direct Injection Engine, Energy Fuels 31 (2017) 4155–4164, doi:10.1021/acs.energyfuels.6b02877.

[3] C. Kolodziej, M. Sellnau, K. Cho, D.A. Best, Operation of a Gasoline Direct Injection Compression Ignition Engine on Naphtha and E10 Gasoline Fuels, SAE Int. J. Engines 9 (2016) 979–1001, doi:10.4271/2016-01-0759.

[4] H. Yamada, S. Inomata, H. Tanimoto, H. Hata, K. Tonokura, Estimation of refueling emissions based on theoretical model and effects of E10 fuel on refueling and evaporative emissions from gasoline cars, Sci. Total Environ. 622–623 (2018) 467–473, doi:10.1016/j.scitotenv.2017.11.339.

[5] R. Zhu, J. Hu, L. He, L. Zu, X. Bao, Y. Lai, S. Su, Effects of ambient temperature on regulated gaseous and particulate emissions from gasoline-, E10- and M15-fueled vehicles, Front. Environ. Sci. Eng. 14 (2021) 1–13, doi:10.1007/s11783-020-1306-1.

[6] K. Katz, M. Newman, Vapor-Liquid Equilibria for Ethyl Alcohol-n-Heptane at Low Pressure, Ind. Eng. Chem. 49 (1956) 137–141, doi:10.1021/ie50553a040.

[7] J.D. Raal, R.K. Code, D.A. Best, Examination of Ethanol-n-Heptane, Methanol-n-Hexane System using New Vapor-Liquid Equilibrium Still, J. Chem. Eng. Data 17 (1972) 211–216, doi:10.1021/je60053a019.

[8] V.R. Bhetanabotla, S.W. Campbell, P-x Measurements for Ethanol-n-Heptane-isobutanol at 303.15K, Fluid Phase Equilib. 62 (1991) 239–258, doi:10.1016/0378-3812(91)80013-L.

[9] A.G. Pradhan, V.R. Bhethanabotla, S.W. Campbell, Vapor-liquid equilibrium data for ethanol-n-heptane-1-propanol and ethanol-n-heptane-2-propanol and their interpretation by a simple association model, Fluid Phase Equilib. 84 (1993) 183–206, doi:10.1016/0378-3812(93)85123-4.

[10] M. Hongo, T. Tsuji, K. Fukuchi, Y. Arai, Vapor-Liquid Equilibria of Methanol + Hexane, Methanol + Heptane, Ethanol + Hexane, Ethanol + Heptane, and Ethanol + Octane at 298.15K, J. Chem. Eng. Data 39 (1994) 688–691, doi:10.1021/je00016a010.

[11] M. Ronc, G.R. Ratcliff, Measurement of vapor-liquid equilibria using a semi-continuous total pressure static equilibrium still, Can. J. Chem. Eng. 54 (1976) 326–332, doi:10.1002/cjce.5450540414.

[12] C. Berro, M. Rogalski, A. Peneloux, A new ebulliometric technique. vapor-liquid equilibria in the binary systems ethanol + n-heptane and ethanol + n-nonane, Fluid Phase Equilib. 8 (1982) 55–73, doi:10.1016/0378-3812(82)80005-8.

[13] G.A. Ratcliff, K.C. Chao, Prediction of thermodynamic properties of polar mixtures by a group solution model, Can. J. Chem. Eng. 47 (1969) 148–153, doi:10.1002/cjce.5450470208.

[14] B. Janaszewski, P. Oracz, M. Goral, S. Warycha, Vapour-liquid equilibria. I. An apparatus for isothermal total vapour pressure measurements: binary mixtures of ethanol and t-butanol with n-hexane, n-heptane and n-octane at 313.15K, Fluid Phase Equilib. 9 (1982) 295–310, doi:10.1016/0378-3812(82)80025-3.

[15] J. Zielkiewicz, (Vapour + liquid) equilibria in (heptane + ethanol + propan-1-ol) at the temperature 313.15K, J. Chem. Thermodyn. 25 (1993) 1077–1082, doi:10.1006/jcht.1993.1105.

[16] R.S. Ramalho, J. Delmas, Isothermal and isobaric vapor-liquid equilibrium data and excess free energies by the total pressure method, J. Chem. Eng. Data 13 (1968) 161–164, doi:10.1021/je60037a005.

[17] J. Seo, S. Lee, H. Kim, Measurement and Correlation of Vapor–Liquid Equilibria for the Ethanol + n-Heptane System near the Critical Region, J. Chem. Eng. Data 47 (2002) 974–977, doi:10.1021/je0200057.

[18] T. Tsuji, T. Sato, T. Hoshina, S. Oba, Boiling Point of Five New -Sulfur Free Odorants for LPG, 1-Pentyne, Cyclopentene, 1-Hexyne, 2-Hexyne and 1,5-Cyclooctadiene, and Bubble Point Pressures of Binaries with Propane, J. Jpn. Petrol. Inst. 64 (2021) 92–102, doi:10.1627/jpi.64.92.

[19] H. Matsuda, M. Negishi, S. Iino, K. Kurihara, K. Tochigi, K. Ochi, J. Gmehling, Isothermal vapor–liquid equilibria at 383.15–413.15K for the binary system methanol + dimethyl carbonate and the pressure dependency of the azeotropic point, Fluid Phase Equilib. 492 (2019) 101–109, doi:10.1016/j.fluid.2019.03.019.

[20] H. Matsuda, K. Inaba, K. Nishihara, H. Sumida, K. Kurihara, K. Tochigi, K. Ochi, Separation Effects of Renewable Solvent Ethyl Lactate on the Vapor-Liquid Equilibria of the Methanol + Dimethyl Carbonate Azeotropic System, J. Chem. Eng. Data 62 (2017) 2944–2952, doi:10.1021/acs.jced.7b00185.

[21] H. Matsuda, K. Inaba, H. Sumida, K. Kurihara, K. Tochigi, K. Ochi, Vapor-liquid equilibria of binary and ternary mixtures containing ethyl lactate and effect of ethyl lactate as entertainer, Fluid Phase Equilib. 420 (2016) 50–57, doi:10.1016/j.fluid.2015.12.029.

[22] H. Taguchi, J. Nakakubo, H. Matsuda, K. Kurihara, K. Tochigi, Determination of vapor-liquid equilibria at elevated pressures using ebulliometer, J. Chem. Eng. Japan 49 (2016) 317–323, doi:10.1252/jcej.14we263.

[23] R. Stryjek, J.H. Vera, PRSV: an Improved Peng-Robinson Equation of State for Pure Compounds and Mixtures, Can. J. Chem. Eng. 64 (1986) 323–333, doi:10.1002/cjce.5450640224.

[24] H. Matsuda, K. Tochigi, K. Kurihara, T. Funazukuri, V.K. Rattan, Estimation of kinematic viscosities at high pressures for binary mixtures CO2 + solvent using modified Eyring–Wilson and McAllister models, Molecular Physics, Mol. Phys. 117 (2019) 3913–3921, doi:10.1080/00268976.2019.1671618.

[25] H. Matsuda, K. Tochigi, K. Kurihara, T. Funazukuri, V.K. Rattan, Estimation of kinematic viscosities for multi-component systems using modified Eyring and activity coefficient model, Fluid Phase Equilib. 492 (2019) 137–144, doi:10.1016/j.fluid.2019.03.017.

[26] H. Matsuda, K. Tochigi, K. Kurihara, T. Funazukuri, V.K. Rattan, Estimation of kinematic viscosities for CO2 expanded liquids by ASOG-VISCO model, Fluid Phase Equilib. 470 (2018) 188–192, doi:10.1016/j.fluid.2018.01.033.

[27] K. Tochigi, T. Okamura, V.K. Rattan, Prediction of high-pressure viscosities for binary liquid mixtures using the EOS-GE mixing rule with low-pressure viscosity data, Fluid Phase Equilib. 257 (2007) 228–232, doi:10.1016/j.fluid.2007.02.032.

[28] T. Ono, M. Kyoda, R. Amezawa, M. Ota, Y. Sato, H. Inomata, Measurement and correlation of density and viscosity of n-alcohol–water mixtures at temperatures up to 618K and at pressures up to 40MPa, Fluid Phase Equilib. 453 (2017) 13–23, doi:10.1016/j.fluid.2017.09.005.

[29] R.R. Brunson, C.H. Byers, Viscosities of Alcohol-Hydrocarbon Systems in the Critical Region: a Dynamic Laser Light Scattering Approach, J. Chem. Eng. Data 34 (1989) 46–52, doi:10.1021/je00055a015.

[30] O.C. Bridgeman, E.W. Aldrich, Vapor Pressure Tables for Water, J. Heat Transf. 86 (1964) 279–286, doi:10.1115/1.3687121.

[31] M.-.J. Huron, J. Vidal, New mixing rules in simple equations of state for representing vapour-liquid equilibria of strongly non-ideal mixtures, Fluid Phase Equilib. 3 (1979) 255–271, doi:10.1016/0378-3812(79)80001-1.

[32] M.L. Michelsen, A modified Huron-Vidal mixing rule for cubic equations of state, Fluid Phase Equilib. 60 (1990) 213–219, doi:10.1016/0378-3812(90)85053-D.

[33] D.S.H. Wong, S.I. Sandler, A theoretically correct mixing rule for cubic equations of state, AIChE J., 38, 671–679, doi:10.1002/aic.690380505.

[34] Y. Adachi, H. Sugie, A New Mixing Rule-Modified Conventional Mixing Rule, Fluid Phase Equilib. 28 (1986) 103–118, doi:10.1016/0378-3812(86)85072-5.

[35] R.E. Powell, W.E. Roseveare, H. Eyring, Diffusion, Thermal Conductivity, and Viscous Flow of Liquids, Ind. Eng. Chem. 33 (1941) 430–435, doi:10.1021/ie50376a003.

[36] J.A. Schroeder, S.G. Penoncello, J.S. Schroeder, A Fundamental Equation of State for Ethanol, J. Phys. Chem. Ref. Data 43 (2014) 043102, doi:10.1063/1.4895394.

[37] https://webbook.nist.gov/chemistry/fluid/ (accessed on 1st Oct. 2021)

[38] A. Fredenslund, J. Gmehling, P. Rasmussen, Vapour-Liquid Equilibria Using UNIFAC a Group-Contribution Method, Elsevier, Amsterdam (1977).

[39] J. Wisniak, J. Ortega, L. Fernández, A fresh look at the thermodynamic consistency of vapour-liquid equilibria data, J. Chem. Thermodyn. 105 (2017) 385–396, doi:10.1016/j.jct.2016.10.038.